

# Analysis of the Hopfield Model Incorporating the Effects of Unlearning

Shuta Takeuchi\*

*Department of Physics, The University of Tokyo,*

*7-3-1 Hongo, Tokyo 113-0033, Japan*

Takashi Takahashi†

*Institute for Physics of Intelligence, The University of Tokyo,*

*7-3-1 Hongo, Tokyo 113-0033, Japan*

Yoshiyuki Kabashima‡

*Institute for Physics of Intelligence, The University of Tokyo,*

*7-3-1 Hongo, Tokyo 113-0033, Japan and*

*Trans-Scale Quantum Science Institute,*

*The University of Tokyo, 7-3-1 Hongo, Tokyo 113-0033, Japan*

(Dated: February 10, 2026)

## Abstract

We analyze a variant of the Hopfield model that incorporates an unlearning mechanism based on spin correlations in the high-temperature regime. In the large system limit where extensively many patterns are stored, we employ the replica method under the replica symmetric ansatz to characterize the model analytically. Our analysis provides a systematic and self-consistent framework that yields order-parameter equations and stability conditions at finite temperatures over a wide range of parameter settings. The resulting theory accurately captures the behavior of the signal-to-noise ratio, the memory capacity, and the criteria for selecting optimal hyperparameters, in agreement with the qualitative findings of Nokura (1996 *J. Phys. A: Math. Gen.* **29** 3871). Moreover, the theoretical predictions show good agreement with numerical simulations, supporting the conclusion that unlearning enhances memory capacity by suppressing spurious memories.

## I. INTRODUCTION

The Hopfield model was originally proposed as a paradigmatic model of associative memory in neural systems [1]. By storing patterns through Hebbian learning, the model enables retrieval via energy minimization in a fully connected network. In the limit where the numbers of neurons  $N$  and stored patterns  $P$  tend to infinity keeping the pattern load  $\alpha = P/N$  finite, the phase structure of the Hopfield model is well understood within the framework of spin-glass theory [2], exhibiting retrieval, spin-glass, and paramagnetic phases. A critical pattern load  $\alpha_c \simeq 0.14$  separates the retrieval phase from the spin-glass phase, beyond which reliable recall of stored patterns becomes impossible.

Even below this critical load, however, the energy landscape of the Hopfield model contains many locally stable states that do not correspond to any single stored pattern. These so-called spurious memories arise from the coexistence of multiple metastable states and can significantly degrade retrieval performance [2]. To address this issue, Hopfield and collaborators introduced the concept of *unlearning*, in which interactions associated with spurious states are selectively weakened [3]. In the original formulation, the network is repeatedly initialized from random configurations and allowed to relax to fixed points, and the resulting

---

\* takesyu1928@g.ecc.u-tokyo.ac.jp

† takashi-takahashi@g.ecc.u-tokyo.ac.jp

‡ kaba@phys.s.u-tokyo.ac.jp

spin configurations are used to modify synaptic couplings via an anti-Hebbian rule. This idea is biologically motivated by the hypothesis that REM sleep serves to eliminate unnecessary or parasitic memories [4].

While the original unlearning scheme relies on information extracted from converged states, its essential purpose is to suppress spurious correlations in the network. Motivated by this observation, several alternative unlearning strategies have been proposed that do not explicitly depend on convergence dynamics. These include pseudo-inverse-type methods [5, 6], eigenvector-based approaches [7], and schemes based on spin correlations evaluated in the high-temperature phase [8]. Both theoretical analyses and numerical simulations have demonstrated that such methods can improve retrieval performance by reducing spurious memories.

In this work, we focus on the unlearning model proposed by Nokura [8], hereafter referred to as the  $J'$  model. In this model, unlearning is implemented by modifying the Hebbian couplings using spin correlation functions computed in the high-temperature phase at inverse temperature  $\gamma \ll 1$ . Previous studies based on signal-to-noise (SN) ratio analysis and numerical simulations have suggested that this mechanism enhances retrieval robustness and increases memory capacity. However, these analyses were primarily qualitative and restricted to the zero-temperature limit. As a consequence, the precise location and nature of the phase boundaries, the dependence of memory capacity on unlearning parameters, and the behavior at finite temperatures have remained unclear.

A quantitative understanding of these issues is essential for evaluating the effectiveness and robustness of unlearning. In particular, the dependence of the memory capacity on the unlearning strength and temperature is crucial for identifying optimal parameter regimes, while finite-temperature analysis is indispensable for understanding the stability of retrieval under noise and thermal fluctuations.

The purpose of this paper is to provide a systematic statistical-mechanics analysis of the  $J'$  model and to clarify the effects of unlearning within a unified theoretical framework. Using the replica method under the replica symmetric (RS) ansatz, we derive the free energy and the corresponding saddle-point equations in the large system limit of  $N \rightarrow \infty$  with finite pattern load  $\alpha$ . We analyze the retrieval performance, phase diagram, and stability conditions at finite temperatures, and compare the theoretical predictions with numerical simulations. Furthermore, we evaluate the signal-to-noise ratio within the replica framework,

confirm consistency with previous qualitative studies, and determine the memory capacity and its dependence on unlearning parameters theoretically.

This paper is organized as follows. In Sec. II, we introduce the  $J'$  model and derive an effective interaction by rewriting the spin-correlation term using a mean-field approximation. In Sec. III, we perform a replica analysis under the RS ansatz and obtain the saddle-point equations. In Sec. IV, we analyze the macroscopic properties of the system, including retrieval performance, signal-to-noise ratio, phase diagrams, and memory capacity. Section V concludes the paper with a summary and discussion of future directions.

## II. MODEL SETUP

In this section, we introduce the  $J'$  model, and derive an effective form of the interaction by rewriting the spin correlation function using a mean-field approximation.

### A. $J'$ model

Let us suppose the same setup as in the Hopfield model for the spins and patterns. The  $J'$  model incorporates unlearning by using the spin correlation function computed in the high-temperature phase of the Hopfield model, as

$$J'_{ij} = \begin{cases} J_{ij} - \epsilon \langle S_i S_j \rangle_\gamma & (i \neq j), \\ 0 & (i = j). \end{cases} \quad (1)$$

Here,  $\epsilon$  is the unlearning strength and  $\gamma$  is the inverse temperature in the high-temperature phase ( $0 < \gamma \ll 1$ ), and  $J_{ij}$  is defined by standard Hebbian rule. The use of the high-temperature spin correlation function is motivated by the expectation that it contains rich information on spurious memories, while being only weakly affected by the retrieval states. With this interaction  $J'$ , the model is defined by

$$H(\mathbf{S}) = -\frac{1}{2} \sum_{i \neq j} J'_{ij} S_i S_j = -\frac{1}{2} \mathbf{S}^\top J' \mathbf{S}, \quad \mathbf{S} = (S_1, \dots, S_N)^\top, \quad (2)$$

$$P(\mathbf{S} | \{\xi^\mu\}) = \frac{\exp(-\beta H(\mathbf{S}))}{\text{Tr} \exp(-\beta H(\mathbf{S}))}. \quad (3)$$

where  $\text{Tr}$  denotes the summation or integration over all possible states. The spin correlation function is computed as

$$\begin{aligned}\langle S_i S_j \rangle_\gamma &= \frac{1}{Z_\gamma} \text{Tr} S_i S_j \exp \left( \frac{\gamma}{2} \sum_{i \neq j} J_{ij} S_i S_j \right) \\ Z_\gamma &= \text{Tr} \exp \left( \frac{\gamma}{2} \sum_{i \neq j} J_{ij} S_i S_j \right).\end{aligned}\quad (4)$$

In the Hopfield framework, stored patterns are expected to be located close to stable configurations (local minima) of the energy function. To study memory retrieval and to compare the analytical results with those of simulations, it is therefore necessary to introduce a concrete dynamics that drives the system toward such energy minima.

## B. Rewriting Interactions by Mean Field Analysis

As it stands in Eq. (1), it is computationally difficult to evaluate the correlation function  $\langle S_i S_j \rangle_\gamma$ . As a practical solution, we assess it by the mean-field approximation. In the high-temperature phase, a mean-field expansion yields

$$\langle S_i S_j \rangle_\gamma = \delta_{ij} + \gamma \sum_k J_{ik} \langle S_k S_j \rangle_\gamma + \dots. \quad (5)$$

for  $0 < \gamma \ll 1$ . This expansion implies that the spin correlation  $\langle S_i S_j \rangle_\gamma$  can be written as

$$\langle S_i S_j \rangle_\gamma \simeq ((I - \gamma J)^{-1})_{ij}. \quad (6)$$

Using this approximation, the interaction of the  $J'$  model is redefined as

$$J' = J - \epsilon (I - \gamma J)^{-1}. \quad (7)$$

In this paper we analyze this model. The diagonal terms of  $J'$  contribute only constants in the replica calculation and are ignored.

Table I summarizes the parameters used in this study.

## III. REPLICA ANALYSIS

In this section, we analyze the  $J'$  model using the replica method. For this purpose, we first evaluate the  $n$ -th moment of the partition function for  $n = 1, 2, \dots \in \mathbb{N}$  introducing

TABLE I. Model parameters used in this study

Symbol	Name	Definition/Role
$\alpha$	Pattern load	Ratio of the number of stored patterns $P$ to neurons $N$
$\epsilon$	Unlearning strength	Strength that weakens Hebbian couplings
$\gamma$	Unlearning inverse temperature	Sets $\langle S_i S_j \rangle_\gamma \approx (I - \gamma J)_{ij}^{-1}$
$\beta$	Physical inverse temperature	Temperature of the analyzed model

auxiliary variables to handle the matrix inversion. Then, we analytically continue the obtained expression of the moment of the partition function to real numbers  $n \in \mathbb{R}$  under the RS ansatz, which yields the average free energy. Finally, we take the zero temperature limit for examining the property of the local minima of the energy function of Eq. (1).

### A. Handling matrix inversion

The partition function to be analyzed is

$$Z = \text{Tr} \exp \left( \frac{\beta}{2} \mathbf{S}^\top J' \mathbf{S} \right) = \text{Tr} \exp \left( \frac{\beta}{2} \mathbf{S}^\top J \mathbf{S} - \frac{\epsilon \beta}{2} \mathbf{S}^\top (I - \gamma J)^{-1} \mathbf{S} \right). \quad (8)$$

To handle the inverse of  $I - \gamma J$ , we introduce a new variable  $\phi$  via a Hubbard–Stratonovich transformation.

$$Z = \int_{-i\infty}^{i\infty} d\phi \text{Tr} \exp \left( \frac{\beta}{2} \mathbf{S}^\top J \mathbf{S} + \frac{\beta}{2} \phi^\top (I - \gamma J) \phi + \beta \sqrt{\epsilon} \mathbf{S}^\top \phi \right) \frac{\det(I - \gamma J)}{(2\pi i)^{N/2}}. \quad (9)$$

Since the factor  $\det(I - \gamma J)$  contributes only a constant to the free energy  $\log Z$ , we neglect it in the following analysis. Neglecting other constant contributions, we will analyze the following

$$\tilde{Z} = \int_{-i\infty}^{i\infty} d\phi \text{Tr} \exp \left( \frac{\beta}{2} \mathbf{S}^\top J \mathbf{S} + \frac{\beta}{2} \phi^\top (I - \gamma J) \phi + \beta \sqrt{\epsilon} \mathbf{S}^\top \phi \right). \quad (10)$$

### B. Replica method

The typical properties of the system can be analyzed by evaluating the configurational average of  $\log \tilde{Z}$  with respect to the stored patterns  $\xi^1, \dots, \xi^P$ . However, a direct evaluation of this quantity is intrinsically difficult.

To overcome this difficulty, we employ the replica method. Within this framework, the disorder average  $\mathbb{E}[\log \tilde{Z}]$  is computed using the identity

$$\mathbb{E}[\log Z] = \lim_{n \rightarrow 0} \frac{\mathbb{E}[Z^n] - 1}{n}, \quad (11)$$

which is evaluated by first computing  $\mathbb{E}[Z^n]$  for natural numbers  $n \in \mathbb{N}$  and then analytically continuing the result to real values  $n \in \mathbb{R}$  [9].

Without loss of generality, we assume that the pattern to be retrieved is  $\boldsymbol{\xi}^1 = \mathbf{1} = (1, 1, \dots, 1)^\top$ . We then evaluate  $\mathbb{E}_{\{\boldsymbol{\xi}^\mu\}}[Z^n]$  by separating the contribution of  $\boldsymbol{\xi}^1$  from those of the remaining patterns. Since all patterns are sampled independently, their contributions factorize. This procedure leads to

$$\begin{aligned} & \mathbb{E}_{\{\boldsymbol{\xi}^\mu\}}[Z^n] \\ &= \text{Tr} \int_{-i\infty}^{i\infty} d\boldsymbol{\phi} \exp \left( \beta \frac{1 + \alpha\gamma}{2} \sum_{i,a} (\phi_i^a)^2 + \beta\sqrt{\epsilon} \sum_{i,a} S_i^a \phi_i^a + \frac{\beta}{2N} \sum_a \left( \sum_i S_i^a \right)^2 - \frac{\beta\gamma}{2N} \sum_a \left( \sum_i \phi_i^a \right)^2 \right) \\ & \quad \times \left( \mathbb{E}_{\boldsymbol{\xi}} \left[ \exp \left( \frac{\beta}{2} \sum_a \left( \frac{1}{\sqrt{N}} \sum_i \xi_i S_i^a \right)^2 - \frac{\beta\gamma}{2} \sum_a \left( \frac{1}{\sqrt{N}} \sum_i \xi_i \phi_i^a \right)^2 \right) \right] \right)^{P-1}, \end{aligned} \quad (12)$$

where we have dropped the pattern index  $\mu = 2, 3, \dots, P$ , since all these patterns give identical contributions.

To perform the average with respect to  $\boldsymbol{\xi}$ , we introduce the variables

$$v_a = \frac{1}{\sqrt{N}} \sum_i \xi_i S_i^a, \quad w_a = \frac{1}{\sqrt{N}} \sum_i \xi_i \phi_i^a.$$

For fixed  $\{S^a, \phi^a\}$ , the central limit theorem implies that  $\{v_a, w_a\}$  follow a multivariate Gaussian distribution with zero mean. Their covariances are determined by the overlaps  $N^{-1} \sum_i S_i^a S_i^b$ ,  $N^{-1} \sum_i \phi_i^a \phi_i^b$ , and  $N^{-1} \sum_i S_i^a \phi_i^b$ . Consequently, Eq. (12) depends on  $\mathbf{S}^a$  and  $\boldsymbol{\phi}^a$  only through macroscopic quantities such as  $N^{-1} \sum_i S_i^a$  and  $N^{-1} \sum_i S_i^a S_i^b$ . This moti-

vates the introduction of the following order parameters:

$$m_a = \frac{1}{N} \sum_i S_i^a, \quad (13)$$

$$u_a = \frac{1}{N} \sum_i \phi_i^a, \quad (14)$$

$$q_{ab} = \frac{1}{N} \sum_i S_i^a S_i^b, \quad (15)$$

$$r_{ab} = \frac{1}{N} \sum_i S_i^a \phi_i^b, \quad (16)$$

$$p_{ab} = \frac{1}{N} \sum_i \phi_i^a \phi_i^b. \quad (17)$$

Here,  $m_a$  represents the overlap with the target pattern  $\xi^1 = \mathbf{1}$ , and  $q_{ab}$  denotes the overlap between replicas  $\mathbf{S}^a$  and  $\mathbf{S}^b$ . The remaining order parameters arise from the introduction of the unlearning mechanism and are absent in the standard Hopfield model.

We enforce these definitions by introducing conjugate variables (denoted by hats) via the Fourier representation of the delta function. For example,

$$\begin{aligned} 1 &= \int d q_{ab} \delta \left( N q_{ab} - \sum_i S_i^a S_i^b \right) \\ &= \int d q_{ab} \int_{-i\infty}^{i\infty} \frac{d \hat{q}_{ab}}{2\pi i} \exp \left( -\hat{q}_{ab} \left( N q_{ab} - \sum_i S_i^a S_i^b \right) \right). \end{aligned} \quad (18)$$

This representation allows all constraints to be expressed in exponential form, which greatly simplifies the analysis.

In the thermodynamic limit  $N, P \rightarrow \infty$  with the pattern load  $\alpha = P/N = \mathcal{O}(1)$ , the disorder-averaged moment of the partition function is dominated by contributions exponential in  $N$ . This enables the use of the saddle-point method, and the configurational average is determined by the extremum of the integrand with respect to the order parameters. Specifically, we obtain

$$\lim_{N \rightarrow \infty} \frac{1}{N} \log \mathbb{E}[\tilde{Z}^n] = -\beta n f,$$

where

$$\begin{aligned} -n\beta f &= -\beta \left( \sum_a (\hat{m}_a m_a + \hat{u}_a u_a) + \sum_{a,b} (\hat{q}_{ab} q_{ab} + \hat{r}_{ab} r_{ab} + \hat{p}_{ab} p_{ab}) \right) \\ &+ \frac{\beta}{2} \sum_a m_a^2 - \frac{\beta\gamma}{2} \sum_a u_a^2 + \alpha \log \int d\mathbf{x} d\mathbf{y} e^{\beta K} + \log \int_{-i\infty}^{i\infty} d\boldsymbol{\phi} \text{Tr} e^{\beta L}, \end{aligned} \quad (19)$$

with

$$L = \frac{1 + \alpha\gamma}{2} \sum_a (\phi^a)^2 + \sqrt{\epsilon} \sum_a S^a \phi^a + \sum_a \hat{m}_a S^a + \sum_a \hat{u}_a \phi^a + \sum_{a,b} \hat{q}_{ab} S^a S^b + \sum_{a,b} \hat{r}_{ab} S^a \phi^b + \sum_{a,b} \hat{p}_{ab} \phi^a \phi^b, \quad (20)$$

$$K = -\frac{i\gamma}{2\beta} \sum_a (x^a)^2 + \frac{i}{2\beta} \sum_a (y^a)^2 + \frac{i\gamma}{2} \sum_{a,b} q_{ab} x^a x^b + \frac{i\gamma}{2} \sum_{a,b} p_{ab} y^a y^b + i\gamma \sum_{a,b} r_{ab} x^a y^b. \quad (21)$$

The saddle-point equations for the order parameters follow from extremizing Eq. (19), and the free energy is obtained by evaluating this expression at the corresponding self-consistent solution. Details of the derivation are provided in Appendix A.

### C. Replica symmetric (RS) ansatz

Without further assumptions on the structure of the saddle point, it is difficult to evaluate Eq. (11), since Eq. (19) still explicitly depends on the discrete replica number  $n$ . The key to resolving this difficulty is to focus on replica symmetry. Because Eq. (19) is invariant under any relabeling or permutation of the replica indices, it is natural to assume that all replicas are equivalent. We therefore impose the following replica-symmetric (RS) ansatz. To simplify the calculation and to match the scaling with  $\beta$ , we parametrize the solution as

$$q_{ab} = \begin{cases} q + \chi_q, & a = b, \\ q, & a \neq b, \end{cases} \quad (22)$$

$$r_{ab} = \begin{cases} r + \chi_r, & a = b, \\ r, & a \neq b, \end{cases} \quad (23)$$

$$p_{ab} = \begin{cases} p + \chi_p, & a = b, \\ p, & a \neq b, \end{cases} \quad (24)$$

$$m_a = m \quad (\forall a), \quad u_a = u \quad (\forall a). \quad (25)$$

For the conjugate variables, we assume

$$\hat{q}_{ab} = \begin{cases} \beta\hat{q} + \hat{\chi}_q, & a = b, \\ \beta\hat{q}, & a \neq b, \end{cases} \quad (26)$$

$$\hat{r}_{ab} = \begin{cases} \beta\hat{r} + \hat{\chi}_r, & a = b, \\ \beta\hat{r}, & a \neq b, \end{cases} \quad (27)$$

$$\hat{p}_{ab} = \begin{cases} \beta\hat{p} + \hat{\chi}_p, & a = b, \\ \beta\hat{p}, & a \neq b, \end{cases} \quad (28)$$

$$\hat{m}_a = \hat{m}, \quad \hat{u}_a = \hat{u} \quad (\forall a). \quad (29)$$

Substituting these expressions into Eq. (19), we obtain

$$\begin{aligned} -\beta f = & -\beta \left( \hat{m}m + \hat{u}u + \beta\hat{q}\chi_q + \hat{\chi}_q q + \hat{\chi}_q\chi_q + \beta\hat{r}\chi_r + \hat{\chi}_r r + \hat{\chi}_r\chi_r + \beta\hat{p}\chi_p + \hat{\chi}_p p + \hat{\chi}_p\chi_p \right) \\ & + \frac{\beta}{2}m^2 - \frac{\beta\gamma}{2}u^2 - \frac{\alpha}{2}\log\Delta + \frac{\alpha\beta}{2\Delta} \left( (1 + \beta\gamma\chi_p)q - \gamma(1 - \beta\chi_q)p - 2\beta\gamma\chi_r r \right) + \beta\hat{\chi}_q \\ & - \frac{1}{2}\log(1 + \alpha\gamma + 2\hat{\chi}_p) - \beta \frac{(\hat{\chi}_r + \sqrt{\epsilon})^2 + \hat{u}^2 + 2\hat{p}}{2(\alpha\gamma + 2\hat{\chi}_p + 1)} \\ & + \int Dy \log 2 \cosh \beta \left( \hat{m} - A\hat{u} + \frac{\delta}{\sqrt{2}}y \right), \end{aligned} \quad (30)$$

where

$$\Delta = (1 - \beta\chi_q)(1 + \beta\gamma\chi_p) + \beta^2\gamma\chi_r^2. \quad (31)$$

The saddle-point equations for the order parameters are then given by

$$m = \int Dy \tanh \beta \left( m + A\gamma u + \frac{\delta}{\sqrt{2}}y \right), \quad (32)$$

$$u = -\frac{1}{\alpha\gamma + 2\hat{\chi}_p + 1} \left( -\gamma u + (\sqrt{\epsilon} + \hat{\chi}_r)m \right), \quad (33)$$

$$q = \int Dy \tanh^2 \beta \left( m + A\gamma u + \frac{\delta}{\sqrt{2}}y \right), \quad \chi_q = 1 - q, \quad (34)$$

$$\chi_p = -\frac{1}{\beta(\alpha\gamma + 2\hat{\chi}_p + 1)} + A^2\chi_q, \quad (35)$$

$$p = \frac{1}{(\alpha\gamma + 2\hat{\chi}_p + 1)^2} \left( \gamma^2 u^2 + 2\hat{p} + 2(\sqrt{\epsilon} + \hat{\chi}_r)(-\gamma mu + \beta\chi_q(\hat{r} - 2\hat{p}A)) + (\sqrt{\epsilon} + \hat{\chi}_r)^2 q \right), \quad (36)$$

$$r = -\frac{1}{\alpha\gamma + 2\hat{\chi}_p + 1} \left( -\gamma um + \beta\chi_q(\hat{r} - 2\hat{p}A) + (\sqrt{\epsilon} + \hat{\chi}_r)q \right), \quad \chi_r = -A\chi_q. \quad (37)$$

The equations for the conjugate variables read

$$\hat{q} = \frac{\alpha}{2\Delta^2} \left( (1 + \beta\gamma\chi_p)^2 q - 2\beta\gamma\chi_r r (1 + \beta\gamma\chi_p) + \beta^2\gamma^2\chi_r^2 p \right), \quad \hat{\chi}_q = \frac{\alpha}{2\Delta} (1 + \beta\gamma\chi_p), \quad (38)$$

$$\hat{p} = \frac{\alpha\gamma^2}{2\Delta^2} \left( \beta^2\chi_r^2 q + 2\beta\chi_r r (1 - \beta\chi_q) + (1 - \beta\chi_q)^2 p \right), \quad \hat{\chi}_p = -\frac{\alpha\gamma}{2\Delta} (1 - \beta\chi_q), \quad (39)$$

$$\hat{r} = \frac{\alpha\gamma}{\Delta^2} \left( -\beta(1 + \beta\gamma\chi_p)\chi_r q - (\Delta - 2\beta^2\gamma\chi_r^2)r + \beta\gamma(1 - \beta\chi_q)\chi_r p \right), \quad \hat{\chi}_r = -\frac{\alpha\beta\gamma}{\Delta} \chi_r, \quad (40)$$

$$\Delta = (1 - \beta\chi_q)(1 + \beta\gamma\chi_p) + \beta^2\gamma\chi_r^2, \quad (41)$$

$$\Delta_2 = 4\hat{q}\hat{p} - \hat{r}^2, \quad (42)$$

$$A = \frac{\hat{\chi}_r + \sqrt{\epsilon}}{\alpha\gamma + 2\hat{\chi}_p + 1}, \quad (43)$$

$$\delta = \sqrt{\frac{(2\hat{q} + \sqrt{\Delta_2} - A\hat{r})^2 + (\hat{r} - 2A\hat{p} - A\sqrt{\Delta_2})^2}{\hat{q} + \hat{p} + \sqrt{\Delta_2}}}. \quad (44)$$

Here we have defined

$$Dy \equiv \frac{e^{-y^2/2}}{\sqrt{2\pi}} dy. \quad (45)$$

The order parameter  $m$  represents the overlap with the retrieved (target) pattern and therefore serves as a measure of retrieval performance. By examining the behavior of  $m$  as a function of the pattern load  $\alpha$ , one can determine whether memory retrieval is successful. From the explicit form of the  $J'$  model, one naturally expects that the standard Hopfield model is recovered in the limits  $\epsilon \rightarrow 0$  or  $\gamma \rightarrow 0$ . Indeed, a straightforward calculation shows that taking either of these limits in the present equations reproduces the RS saddle-point equations of the Hopfield model.

#### D. Zero Temperature ( $\beta \rightarrow \infty$ ) Expression

The zero-temperature limit ( $\beta \rightarrow \infty$ ) corresponds to the fixed point of the deterministic sequential update dynamics of the Hopfield model, where thermal fluctuations are absent and the system evolves solely through energy minimization. It is therefore useful to derive the saddle-point equations in the limit  $\beta \rightarrow \infty$ .

As  $\beta \rightarrow \infty$ , one has  $q \rightarrow 1$  and  $\chi_q, \chi_p, \chi_r \rightarrow 0$ . In this limit, we assume the standard scaling  $\beta\chi_q = \mathcal{O}(1)$ ,  $\beta\chi_p = \mathcal{O}(1)$ , and  $\beta\chi_r = \mathcal{O}(1)$ . We thus introduce the rescaled variables

$$C \equiv \beta\chi_q, \quad E \equiv \beta\chi_p, \quad F \equiv \beta\chi_r.$$

Taking the limit  $\beta \rightarrow \infty$  under this scaling, the saddle-point equations reduce to

$$m = \operatorname{erf}\left(\frac{m + A\gamma u}{\delta}\right), \quad (46)$$

$$u = -\frac{1}{\alpha\gamma + 2\hat{\chi}_p + 1} (-\gamma u + (\sqrt{\epsilon} + \hat{\chi}_r)m), \quad (47)$$

$$C = \frac{2}{\delta\sqrt{\pi}} \exp\left(-\frac{(m + A\gamma u)^2}{\delta^2}\right), \quad (48)$$

$$p = \frac{1}{(\alpha\gamma + 2\hat{\chi}_p + 1)^2} \left( \gamma^2 u^2 + 2\hat{p} + 2(\sqrt{\epsilon} + \hat{\chi}_r)(-\gamma um + C(\hat{r} - 2\hat{p}A)) + (\sqrt{\epsilon} + \hat{\chi}_r)^2 \right), \quad (49)$$

$$r = -\frac{1}{\alpha\gamma + 2\hat{\chi}_p + 1} (-\gamma um + C(\hat{r} - 2\hat{p}A) + (\sqrt{\epsilon} + \hat{\chi}_r)), \quad (50)$$

$$\hat{q} = \frac{\alpha}{2\Delta^2} \left( (1 + \gamma E)^2 - 2\gamma Fr(1 + \gamma E) + \gamma^2 F^2 p \right), \quad \hat{\chi}_q = \frac{\alpha}{2\Delta} (1 + \gamma E), \quad (51)$$

$$\hat{p} = \frac{\alpha\gamma^2}{2\Delta^2} \left( F^2 + 2Fr(1 - C) + (1 - C)^2 p \right), \quad \hat{\chi}_p = -\frac{\alpha\gamma}{2\Delta} (1 - C), \quad (52)$$

$$\hat{r} = \frac{\alpha\gamma}{\Delta^2} \left( -(1 + \gamma E)F - (\Delta - 2\gamma F^2)r + \gamma(1 - C)Fp \right), \quad \hat{\chi}_r = -\frac{\alpha\gamma}{\Delta} F, \quad (53)$$

$$\Delta = (1 - C)(1 + \gamma E) + \gamma F^2, \quad (54)$$

$$\Delta_2 = 4\hat{q}\hat{p} - \hat{r}^2, \quad (55)$$

$$A = \frac{\hat{\chi}_r + \sqrt{\epsilon}}{\alpha\gamma + 2\hat{\chi}_p + 1}, \quad (56)$$

$$E = -\frac{1}{\alpha\gamma + 2\hat{\chi}_p + 1} + \frac{(\hat{\chi}_r + \sqrt{\epsilon})^2 C}{(\alpha\gamma + 2\hat{\chi}_p + 1)^2}, \quad (57)$$

$$F = -\frac{\hat{\chi}_r + \sqrt{\epsilon}}{\alpha\gamma + 2\hat{\chi}_p + 1} C, \quad (58)$$

$$\delta = \sqrt{\frac{(2\hat{q} + \sqrt{\Delta_2} - A\hat{r})^2 + (\hat{r} - 2A\hat{p} - A\sqrt{\Delta_2})^2}{\hat{q} + \hat{p} + \sqrt{\Delta_2}}}. \quad (59)$$

Here, the error function is defined as

$$\operatorname{erf}(x) = \frac{2}{\sqrt{\pi}} \int_0^x dt e^{-t^2}. \quad (60)$$

#### IV. PERFORMANCE ANALYSIS

In this section, we quantitatively evaluate the effect of unlearning by numerically solving the saddle-point equations derived in the previous section. The validity of the theoretical predictions is assessed through a comparison with numerical simulations. In particular, we use the overlap  $m$ , obtained from Eqs. (32) and (46), as a measure of retrieval performance.

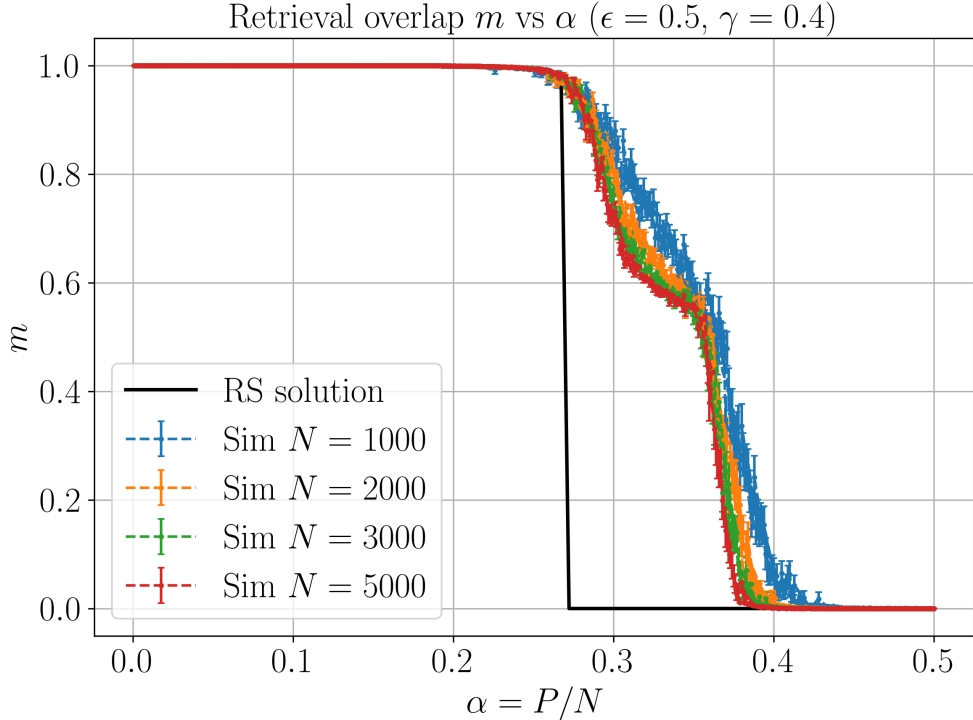


FIG. 1. Overlap  $m$  versus  $\alpha$  at  $\epsilon = 0.5$  and  $\gamma = 0.4$ . Black line: theoretical prediction. Colored lines: direct numerical simulations. Error bars are estimated from 50 independent trials.

### A. Comparison with Numerical Simulations

We compare the results obtained from the replica method with numerical simulations in order to validate our RS calculation.

A simple and commonly used choice for the retrieval dynamics is the asynchronous dynamics in which a single spin is aligned with its local field per update, which guarantees that the system converges to a local minimum of the energy. Instead, we adopted the following synchronous (parallel) update rule:

$$\mathbf{S}^t = \text{sgn}(\mathbf{J}' \mathbf{S}^{t-1}). \quad (t = 1, 2, \dots) \quad (61)$$

where  $\mathbf{S}^t = (S_1^t, S_2^t, \dots, S_N^t)^\top$  and  $S_i^t$  is the state of spin  $i$  at step  $t$ . Unlike the asynchronous updates, a monotonic decrease of the energy at each step is not generally guaranteed for the synchronous updates. Nevertheless, in practice, the synchronous dynamics typically converges to a locally stable fixed point that corresponds to a local minimum of the energy with lower computational costs than the asynchronous dynamics.

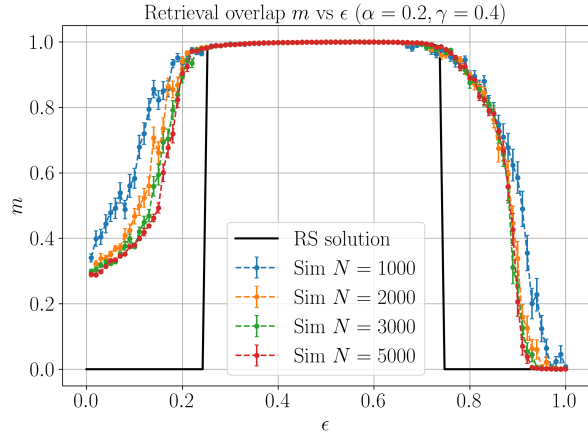


FIG. 2.  $m$  versus  $\epsilon$  at  $\alpha = 0.2$  and  $\gamma = 0.4$ .

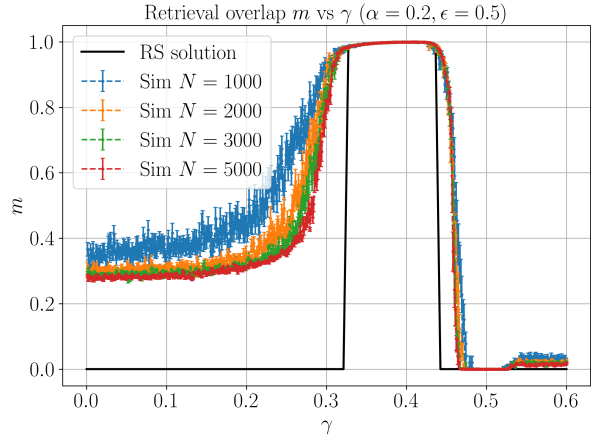


FIG. 3.  $m$  versus  $\gamma$  at  $\alpha = 0.2$  and  $\epsilon = 0.5$ .

Figure 1 shows the dependence of  $m$  on  $\alpha$  for  $\epsilon = 0.5$  and  $\gamma = 0.4$ . Our theoretical prediction agrees well with the numerical simulations in the retrieval phase. The resulting memory capacity is  $\alpha_c(\epsilon = 0.5, \gamma = 0.4) \simeq 0.272$ , confirming that unlearning improves retrieval performance.

Above the transition point, the theoretical analysis predicts a spin-glass phase in which the overlap vanishes,  $m = 0$ , while the spin-glass order parameter remains finite,  $q \neq 0$ . In contrast, numerical simulations clearly show a nonzero overlap. This discrepancy can be attributed to the difference between the equilibrium analysis based on the replica method and the zero-temperature synchronous dynamics employed in the simulations. The replica calculation characterizes the thermodynamic equilibrium state, for which the overlap vanishes in the spin-glass phase. By contrast, synchronous updates do not necessarily converge to equilibrium; depending on the initial condition and the update trajectory, the dynamics may relax to a locally stable configuration that is not representative of the equilibrium state. As a result, simulations can exhibit a finite overlap even in regions where the equilibrium theory predicts  $m = 0$ , reflecting the properties of the update dynamics rather than the equilibrium behavior of the model.

Next, we fix  $\alpha = 0.2$  and vary the unlearning parameters  $\epsilon$  and  $\gamma$ . Figures 2 and 3 show the dependence of the overlap  $m$  on  $\epsilon$  and  $\gamma$ , respectively. Theoretical predictions and numerical simulations are in good agreement within the retrieval phase. Moreover,  $m$  exhibits a first-order phase transition as a function of the unlearning parameters, indicating that the effectiveness of unlearning is highly sensitive to the choice of  $\epsilon$  and  $\gamma$ .

## B. Signal-to-Noise (SN) Ratio

In Ref. [8], Nokura analyzed the present model using a qualitative argument based on a signal-to-noise (SN) analysis. Here we briefly review this argument and then reformulate it within our theoretical framework.

We first examine the stability of the state in which the spins are aligned exactly with the first stored pattern,  $\mathbf{S} = \boldsymbol{\xi}^1$ . In this situation, the local field acting on site  $i$  is given by

$$\begin{aligned} h_i &= \sum_{j \neq i} J'_{ij} \xi_j^1 \\ &= \sum_{j \neq i} J_{ij} \xi_j^1 - \epsilon \sum_{j \neq i} \langle S_i S_j \rangle_\gamma \xi_j^1. \end{aligned} \quad (62)$$

From the update dynamics in Eq. (61), one expects that the pattern  $\boldsymbol{\xi}^1$  is stable if  $\xi_i^1 h_i$  is positive for all, or at least for almost all, sites. To analyze this condition, the local field  $h_i$  is decomposed into a signal component, proportional to  $\xi_i^1$ , and a noise component that is uncorrelated with  $\xi_i^1$ ,

$$h_i = h_s \xi_i^1 + h_n. \quad (63)$$

Substituting the Hebbian coupling into Eq. (62) and extracting the terms proportional to  $\xi_i^1$  by performing a high-temperature expansion of the spin correlation function, Nokura obtained the signal term

$$h_s = 1 - \frac{\epsilon \gamma}{1 - \gamma}. \quad (64)$$

The magnitude of the noise term is estimated as

$$|h_n| \sim \sqrt{\left(1 - \frac{\epsilon \gamma}{(1 - \gamma)^2}\right)^2 \alpha + \frac{\epsilon^2}{(1 - \gamma)^2} \frac{A^2}{1 - A}}, \quad (65)$$

where  $A = \alpha \gamma^2 / (1 - \gamma)^2$ . The ratio  $(h_s/h_n)^2$  thus serves as an indicator of memory performance: when it is large, the signal dominates over the noise and the pattern is stable, whereas when it is small, retrieval fails. This criterion provides a qualitative assessment of the effect of unlearning.

Following this approach, we now examine the SN ratio within our theoretical framework, based on the saddle-point equations derived in the previous sections. The overlap  $m$  is

determined by

$$m = \int Dy \tanh \beta \left( \hat{m} - A\hat{u} + \frac{\delta}{\sqrt{2}}y \right), \quad (66)$$

where the argument of the hyperbolic tangent can be interpreted as an effective field acting on a typical spin. In direct analogy with Nokura's argument, we decompose this effective field into a deterministic part and a fluctuating noise part. The term  $\delta y/\sqrt{2}$  represents the cross-talk noise generated by the non-retrieved patterns, while the remaining contribution corresponds to the systematic field associated with the retrieved pattern.

Using

$$\hat{u} = \gamma \frac{\sqrt{\epsilon} + \hat{\chi}_r}{1 + \alpha\gamma + 2\hat{\chi}_p - \gamma} m, \quad \hat{m} = m, \quad (67)$$

the noise-free component of the effective field,  $\hat{m} - A\hat{u}$ , plays the role of the signal  $h_s$  in Nokura's terminology. Similarly, the fluctuation amplitude  $\delta/\sqrt{2}$  is identified with the noise strength  $h_n$ . We therefore define

$$\begin{aligned} h_s &= 1 - A\gamma \frac{\sqrt{\epsilon} + \hat{\chi}_r}{1 + \alpha\gamma + 2\hat{\chi}_p - \gamma} \\ &= 1 - \gamma \frac{(\hat{\chi}_r + \sqrt{\epsilon})^2}{(1 + \alpha\gamma + 2\hat{\chi}_p - \gamma)(1 + \alpha\gamma + 2\hat{\chi}_p)}, \end{aligned} \quad (68)$$

$$h_n = \frac{\delta}{\sqrt{2}} = \sqrt{\frac{(2\hat{q} + \sqrt{\Delta_2} - A\hat{r})^2 + (\hat{r} - 2A\hat{p} - A\sqrt{\Delta_2})^2}{2\hat{q} + 2\hat{p} + 2\sqrt{\Delta_2}}}. \quad (69)$$

This definition enables a direct and quantitative comparison with the SN-ratio analysis of Nokura within a unified framework.

Figure 4 shows that unlearning enhances the SN ratio compared to the Hopfield model. The result of Ref. [8] (orange curve) agrees well with our calculation below the transition point. Our analysis thus confirms the theoretical improvement of the SN ratio and reproduces the earlier qualitative argument. However, the discontinuous jump at the transition point is not captured in Ref. [8], reflecting the limitations of the qualitative SN analysis.

### C. Phase diagram and AT Line

Another advantage of the present approach over the previous SN analysis is that it enables us to construct phase diagrams while explicitly taking finite-temperature effects into account.

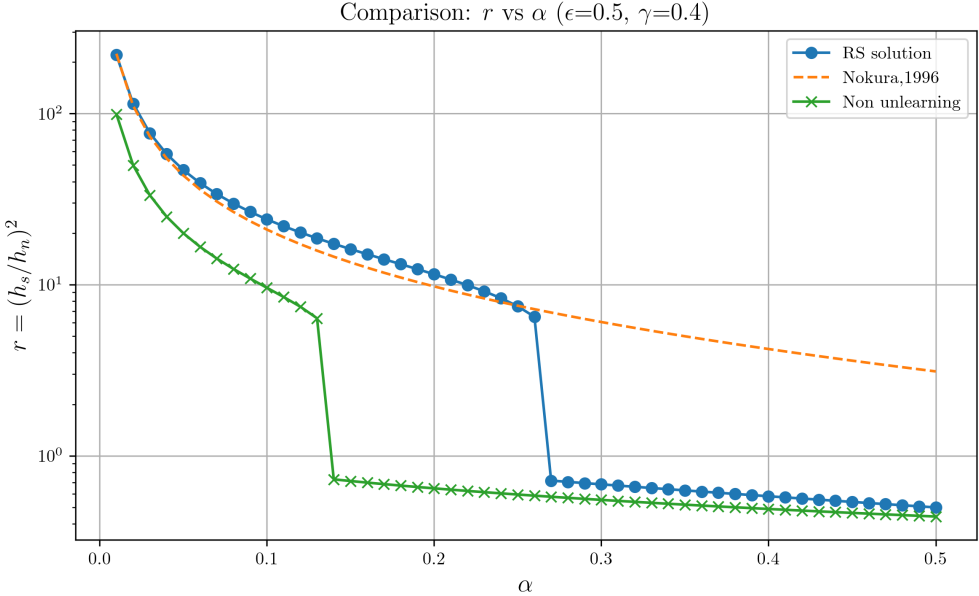


FIG. 4. Signal-to-noise ratio at  $\epsilon = 0.5$  and  $\gamma = 0.4$ . Blue: present theoretical result. Green: Hopfield model. Orange: SN-ratio analysis of Ref. [8].

By numerically solving the saddle-point equations at finite temperature, we obtain the finite-temperature phase diagram shown in Fig. 5.

Unlearning reduces the overall magnitude of the effective interactions, which results in a rescaling of the temperature axis in the phase diagram. To account for this effect and to allow for a meaningful comparison on a common vertical scale, we introduce a normalization constant  $\tilde{J}$  and rescale the temperature as  $T/\tilde{J}$ . We define  $\tilde{J}$  as

$$\tilde{J} = \frac{1 - \epsilon\gamma - \gamma}{1 - \gamma}.$$

This expression is obtained by substituting the Hebbian interaction for a single stored pattern into the definition of  $J'$  in Eq. (7), evaluating the resulting effective coupling, and comparing it with the original Hopfield interaction  $J$ .

In Fig. 5, the black solid line and the green dashed line indicate the reference phase boundaries of the Hopfield model without unlearning. The black line corresponds to the boundary between stable and metastable retrieval states, while the green line denotes the boundary between the retrieval and spin-glass phases. Compared to these reference lines, both boundaries extend to larger values of the pattern load  $\alpha$  in the presence of unlearning. Moreover, the spin-glass region is significantly reduced, indicating an effective suppression

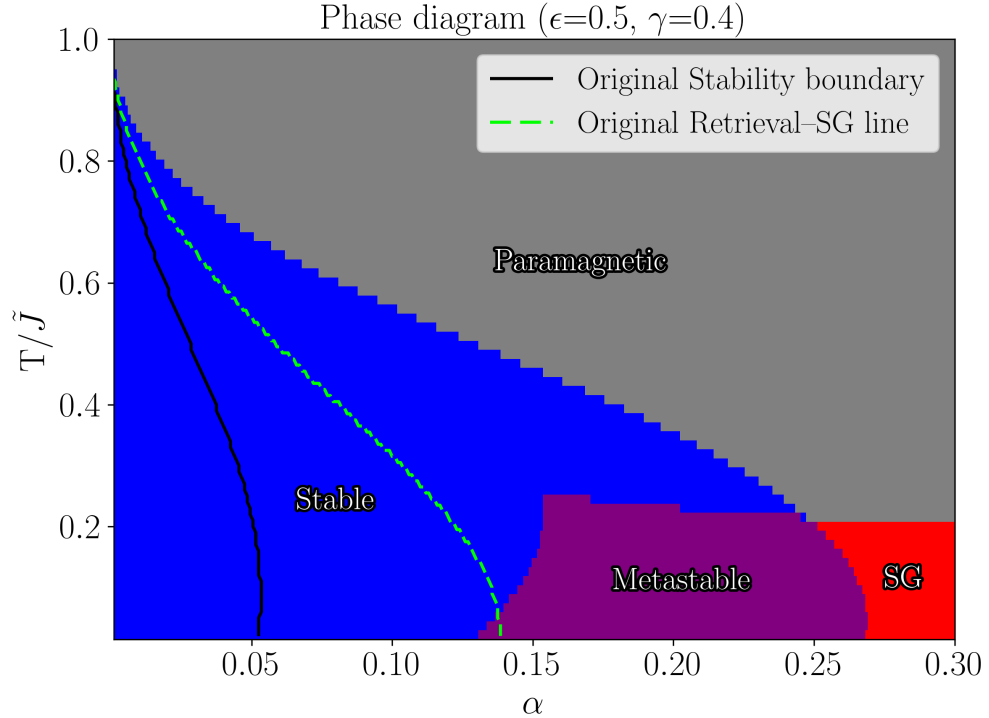


FIG. 5. Phase diagram at  $\epsilon = 0.5$  and  $\gamma = 0.4$ . The blue and purple regions correspond to the retrieval phase: blue indicates a stable retrieval state, while purple denotes a metastable one. The gray region represents the paramagnetic phase, and the red region the spin-glass (SG) phase. The constant  $\tilde{J}$  is a scaling factor for the temperature.

of spurious memories. On the other hand, as indicated by the purple region, there exists a finite temperature above which the metastable part of the retrieval phase disappears.

This disappearance of the metastable retrieval phase at finite temperature does not occur in the standard Hopfield model without unlearning. At present, the detailed mechanism underlying this behavior remains unclear.

To investigate the stability of the RS solution, we introduce a one-step replica symmetry breaking (1RSB) perturbation and evaluate the stability against small deviations. This procedure yields the de Almeida-Thouless (AT) condition [10]. The details of the calculation are provided in Appendix B; here we only summarize the result. We define the following

two matrices:

$$U = \begin{bmatrix} \frac{\alpha}{2\Delta^2}(1 + \beta\gamma\chi_p)^2 & \frac{\alpha}{2\Delta^2}(-2\beta\gamma\chi_r)(1 + \beta\gamma\chi_p) & \frac{\alpha}{2\Delta^2}(\beta\gamma\chi_r)^2 \\ \frac{\alpha\gamma}{\Delta^2}(-\beta\chi_r)(1 + \beta\gamma\chi_p) & \frac{\alpha\gamma}{\Delta^2}[-(1 + \beta\gamma\chi_p)(1 - \beta\chi_q) + (\beta\gamma\chi_r)^2] & \frac{\alpha\gamma}{\Delta^2}(\beta\gamma\chi_r)(1 - \beta\chi_q) \\ \frac{\alpha\gamma^2}{2\Delta^2}(\beta\chi_r)^2 & \frac{\alpha\gamma^2}{\Delta^2}(\beta\chi_r)(1 - \beta\chi_q) & \frac{\alpha\gamma^2}{2\Delta^2}(1 - \beta\chi_q)^2 \end{bmatrix},$$

and

$$V = \begin{bmatrix} 2\beta^2\mathbb{E}_4 & -2\beta^2\mathbb{E}_4 A & 2\beta^2\mathbb{E}_4 A^2 \\ -2\beta^2\mathbb{E}_4 A & 2\beta^2\mathbb{E}_4 A^2 - \frac{\beta\chi_q}{1 + \alpha\gamma + 2\hat{\chi}_p} & -2\beta^2\mathbb{E}_4 A^3 + \frac{2\beta A\chi_q}{1 + \alpha\gamma + 2\hat{\chi}_p} \\ 2\beta^2\mathbb{E}_4 A^2 & -2\beta^2\mathbb{E}_4 A^3 + \frac{2\beta A\chi_q}{1 + \alpha\gamma + 2\hat{\chi}_p} & 2\beta^2\mathbb{E}_4 A^4 + \frac{2}{(1 + \alpha\gamma + 2\hat{\chi}_p)^2} - \frac{4\beta A^2\chi_q}{1 + \alpha\gamma + 2\hat{\chi}_p} \end{bmatrix}.$$

For compactness, we have defined

$$\mathbb{E}_4 \equiv \mathbb{E}_z \left[ \left( 1 - \tanh^2 \beta \tilde{H}(z_1, z_2) \right)^2 \right].$$

The RS solution is locally unstable if and only if the largest eigenvalue of either  $UV$  or  $VU$  is greater than or equal to unity. Figure 6 shows its critical condition known as the AT line. As in the standard Hopfield model, the AT instability appears only at very low temperatures.

#### D. Heat Map of Memory Capacity

In this subsection, we systematically investigate the memory capacity  $\alpha_c$  as a function of the parameters  $\epsilon$  and  $\gamma$ . Figure 7 presents the results as a heatmap, where the horizontal and vertical axes represent  $\gamma$  and  $\epsilon$ , respectively. We compute the capacity  $\alpha_c$  at each point in this parameter space. As shown in the figure, there is a distinct, crescent-shaped region of high capacity (indicated in yellow), suggesting that the performance of unlearning is highly sensitive to the choice of  $\epsilon$  and  $\gamma$ .

The white dashed curve indicates the trajectory in the  $(\epsilon, \gamma)$  plane that maximizes the signal-to-noise ratio, as proposed in Ref. [8]. This theoretical curve shows excellent agreement with our numerical results in the small- $\gamma$  regime.

Motivated by these observations, we simplify the saddle-point equations in the regime where  $\gamma \ll 1$  and  $\epsilon \gg 1$ , leading to the relation  $\epsilon \simeq 1/\gamma - 2 - \alpha$ . When the parameters

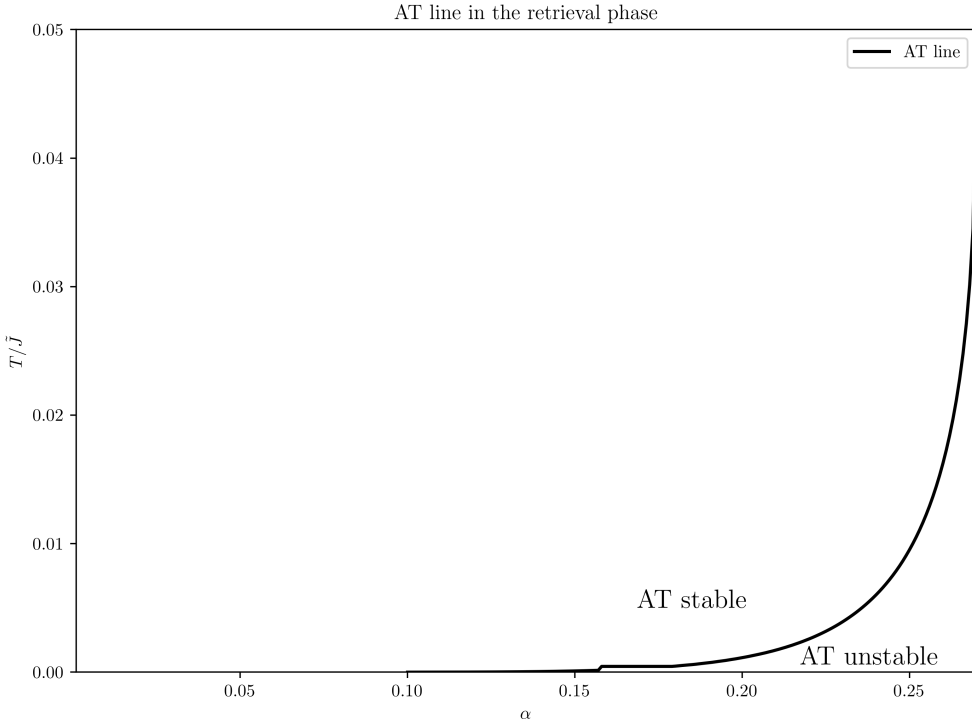


FIG. 6. AT line at  $\epsilon = 0.5$  and  $\gamma = 0.4$ . Numerical simulations were performed in the temperature range  $T \geq 10^{-4}$ .

deviate from this regime, the retrieval performance tends to deteriorate, further highlighting the sensitivity of the system to  $(\epsilon, \gamma)$ . By applying this relation to a small- $\gamma$  expansion of  $J'$ , we reproduce the result in [8],  $J' = \gamma((2 + \alpha)J - J^2)$ . This result suggests that the  $J^2$  term plays a dominant role in the unlearning process. The detailed replica calculation for this framework is provided in Appendix C.

## V. CONCLUSION

In this paper, we presented a systematic statistical-mechanics analysis of a Hopfield model incorporating unlearning based on spin correlations evaluated in the high-temperature regime. Focusing on the  $J'$  model proposed by Nokura, we analyzed the model in the thermodynamic limit using the replica method under the replica-symmetric (RS) ansatz and derived the corresponding free energy and self-consistent saddle-point equations.

Our analysis provides a unified theoretical framework for evaluating the effects of unlearning at both zero and finite temperatures. Within this framework, we clarified how unlearning

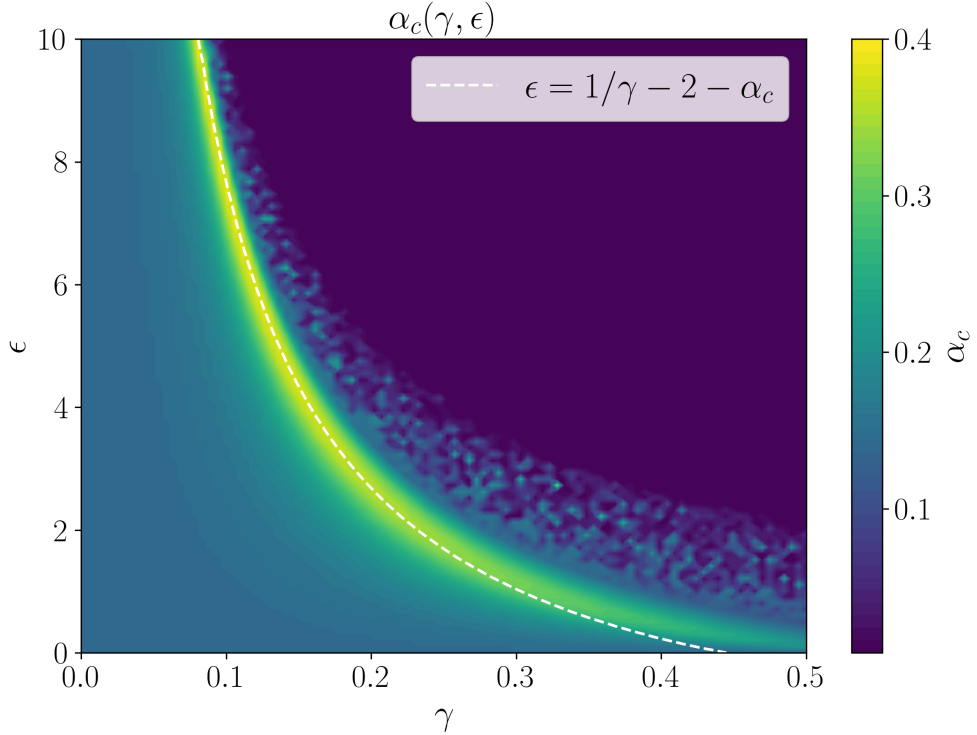


FIG. 7. Memory capacity  $\alpha_c$  for various values of  $\epsilon$  and  $\gamma$ .

modifies the macroscopic order parameters, enhances the signal-to-noise ratio, and increases the memory capacity by suppressing spurious memories. The resulting phase diagrams show that unlearning significantly reduces the spin-glass region and expands the parameter range in which retrieval states are stable. These findings are consistent with, and extend beyond, the earlier qualitative analysis of Nokura, providing a quantitative characterization of the memory capacity and its dependence on the unlearning parameters.

The theoretical predictions obtained from the replica analysis were shown to be in good agreement with numerical simulations in the retrieval phase. This agreement supports the validity of the equilibrium analysis and confirms that unlearning effectively reshapes the energy landscape to favor retrieval states. At finite temperatures, we further identified a metastable retrieval region whose disappearance at higher temperatures is a distinctive feature of the unlearning model and is absent in the standard Hopfield model.

Several open issues remain for future work. A more precise analysis of the zero-temperature limit, including the effects of replica-symmetry breaking, would be necessary to fully characterize the spin-glass phase and the stability of retrieval states. In addition, a dynamical analysis based on dynamical mean-field theory would be useful for understanding

the behavior of synchronous update dynamics and its relation to equilibrium predictions. Extensions of the present framework to generalized associative memory models with higher-order interactions, such as modern Hopfield-type models, also constitute an interesting direction for further study.

## ACKNOWLEDGMENTS

This research was supported by Forefront Physics and Mathematics Program to Drive Transformation (FoPM), a World-leading Innovative Graduate Study (WINGS) Program, the University of Tokyo (ST), MEXT/JSPS KAKENHI Grant No. 22H05117 (YK), JSPS KAKENHI Grant No. 23K16960 and JST ACT-X Grant Number JPMJAX24CG (TT).

## Appendix A: Detailed Calculations of the Replica Method

To evaluate the last term in Eq. (12), we introduce the variables

$$v^a = \frac{1}{\sqrt{N}} \sum_i \xi_i S_i^a, \quad w^a = \frac{1}{\sqrt{N}} \sum_i \xi_i \phi_i^a. \quad (\text{A1})$$

Since  $v^a$  and  $w^a$  are sums of independent random variables, the central limit theorem applies. Accordingly,  $(v^a, w^a)$  are jointly Gaussian with

$$\mathbb{E}[v^a] = \mathbb{E}[w^a] = 0, \quad (\text{A2})$$

$$\mathbb{E}[v^a v^b] = \frac{1}{N} \sum_i S_i^a S_i^b \equiv q_{ab}, \quad (\text{A3})$$

$$\mathbb{E}[v^a w^b] = \frac{1}{N} \sum_i S_i^a \phi_i^b \equiv r_{ab}, \quad (\text{A4})$$

$$\mathbb{E}[w^a w^b] = \frac{1}{N} \sum_i \phi_i^a \phi_i^b \equiv p_{ab}. \quad (\text{A5})$$

These covariances can be summarized in the block form

$$\Sigma = \begin{pmatrix} Q & R \\ R & P \end{pmatrix}, \quad (\text{A6})$$

where  $Q = (q_{ab})$ ,  $R = (r_{ab})$ , and  $P = (p_{ab})$ . Replacing the average over the random patterns  $\xi$  by an average over Gaussian variables  $(\mathbf{v}, \mathbf{w}) \sim \mathcal{N}(0, \Sigma)$ , we obtain

$$\begin{aligned} & \mathbb{E}_\xi \left[ \exp \left( \frac{\beta}{2N} \sum_a \left( \sum_i \xi_i S_i^a \right)^2 - \frac{\beta\gamma}{2N} \sum_a \left( \sum_i \xi_i \phi_i^a \right)^2 \right) \right] \\ &= \mathbb{E}_{(\mathbf{v}, \mathbf{w}) \sim \mathcal{N}(0, \Sigma)} \left[ \exp \left( \frac{\beta}{2} \sum_a (v^a)^2 - \frac{\beta\gamma}{2} \sum_a (w^a)^2 \right) \right]. \end{aligned} \quad (\text{A7})$$

We next introduce the macroscopic order parameters

$$m_a = \frac{1}{N} \sum_i S_i^a, \quad u_a = \frac{1}{N} \sum_i \phi_i^a, \quad (\text{A8})$$

and enforce their definitions, together with those of  $q_{ab}$ ,  $r_{ab}$ , and  $p_{ab}$ , by introducing conjugate variables via the Fourier representation of the delta function (Eq. (18)). This procedure leads to an integral representation of  $\mathbb{E}[Z^n]$  of the form

$$\begin{aligned} \mathbb{E}[Z^n] &= \int \exp \left\{ -N \left( \beta \sum_a (\hat{m}_a m_a + \hat{u}_a u_a) + \beta \sum_{a,b} (\hat{q}_{ab} q_{ab} + \hat{r}_{ab} r_{ab} + \hat{p}_{ab} p_{ab}) \right. \right. \\ &\quad \left. \left. - \frac{\beta}{2} \sum_a m_a^2 + \frac{\beta\gamma}{2} \sum_a u_a^2 \right) \right\} \\ &\times \left( \mathbb{E}_{(\mathbf{v}, \mathbf{w}) \sim \mathcal{N}(0, \Sigma)} \left[ \exp \left( \frac{\beta}{2} \sum_a (v^a)^2 - \frac{\beta\gamma}{2} \sum_a (w^a)^2 \right) \right] \right)^{P-1} \\ &\times \text{Tr} \int_{-i\infty}^{i\infty} \prod_a d\phi^a \exp \left( \beta \frac{1+\alpha\gamma}{2} \sum_{i,a} (\phi_i^a)^2 + \beta\sqrt{\epsilon} \sum_{i,a} S_i^a \phi_i^a \right. \\ &\quad \left. + \beta \sum_a \hat{m}_a \sum_i S_i^a + \beta \sum_a \hat{u}_a \sum_i \phi_i^a + \beta \sum_{a,b} \hat{q}_{ab} \sum_i S_i^a S_i^b \right. \\ &\quad \left. + \beta \sum_{a,b} \hat{r}_{ab} \sum_i S_i^a \phi_i^b + \beta \sum_{a,b} \hat{p}_{ab} \sum_i \phi_i^a \phi_i^b \right). \end{aligned} \quad (\text{A9})$$

For brevity, we do not write the integrations over the order parameters and their conjugates explicitly; in the thermodynamic limit they are evaluated by the saddle-point method.

With these conjugate variables, the couplings between different sites are removed, so that the trace factorizes over  $i$ . The single-site contribution can be written as

$$\begin{aligned} L &= \frac{1+\alpha\gamma}{2} \sum_a (\phi^a)^2 + \sqrt{\epsilon} \sum_a S^a \phi^a + \sum_a \hat{m}_a S^a + \sum_a \hat{u}_a \phi^a + \sum_{a,b} \hat{q}_{ab} S^a S^b \\ &\quad + \sum_{a,b} \hat{r}_{ab} S^a \phi^b + \sum_{a,b} \hat{p}_{ab} \phi^a \phi^b, \end{aligned} \quad (\text{A10})$$

and hence the remaining contribution factorizes as

$$\left( \int_{-i\infty}^{i\infty} \prod_a d\phi^a \text{Tr } e^{\beta L} \right)^N. \quad (\text{A11})$$

We now evaluate the Gaussian expectation over  $(\mathbf{v}, \mathbf{w})$  with covariance matrix  $\Sigma$ . Using the standard formula for Gaussian integrals, we obtain

$$\begin{aligned} & \mathbb{E}_{(\mathbf{v}, \mathbf{w}) \sim \mathcal{N}(0, \Sigma)} \left[ \exp \left( \frac{\beta}{2} \sum_a (v^a)^2 - \frac{\beta\gamma}{2} \sum_a (w^a)^2 \right) \right] \\ &= \left( \det \left[ I - \Sigma \begin{pmatrix} \beta I & 0 \\ 0 & -\beta\gamma I \end{pmatrix} \right] \right)^{-\frac{1}{2}}, \end{aligned} \quad (\text{A12})$$

where the determinant is understood by analytic continuation if necessary. Rewriting the determinant yields

$$= \left( \det \begin{pmatrix} \frac{I}{\beta} - Q & -R \\ -R & -\frac{I}{\beta\gamma} - P \end{pmatrix} \det \begin{pmatrix} \beta I & 0 \\ 0 & -\beta\gamma I \end{pmatrix} \right)^{-\frac{1}{2}}. \quad (\text{A13})$$

For the subsequent saddle-point analysis, it is convenient to apply an analytic continuation and rewrite this as

$$= \left( \det \begin{pmatrix} \frac{iI}{\beta} - iQ & -iR \\ -iR & -\frac{iI}{\beta\gamma} - iP \end{pmatrix} \det \begin{pmatrix} \beta I & 0 \\ 0 & \beta\gamma I \end{pmatrix} \right)^{-\frac{1}{2}}. \quad (\text{A14})$$

Taking the logarithm and dropping additive constants that do not affect the saddle-point equations, we obtain

$$\begin{aligned} & \log \mathbb{E}_{(\mathbf{v}, \mathbf{w}) \sim \mathcal{N}(0, \Sigma)} \left[ \exp \left( \frac{\beta}{2} \sum_a (v^a)^2 - \frac{\beta\gamma}{2} \sum_a (w^a)^2 \right) \right] \\ &= -\frac{1}{2} \log \det \begin{pmatrix} \frac{iI}{\beta} - iQ & -iR \\ -iR & -\frac{iI}{\beta\gamma} - iP \end{pmatrix} + \text{const.} \end{aligned} \quad (\text{A15})$$

Using a Gaussian integral representation of the determinant, this can be rewritten as

$$\begin{aligned} &= \log \int d\mathbf{x} d\mathbf{y} \exp \left[ -\frac{i\gamma}{2\beta} \sum_a (x^a)^2 + \frac{i}{2\beta} \sum_a (y^a)^2 + \frac{i\gamma}{2} \sum_{a,b} q_{ab} x^a x^b + \frac{i\gamma}{2} \sum_{a,b} p_{ab} y^a y^b + i\gamma \sum_{a,b} r_{ab} x^a y^b \right] \\ &= \log \int d\mathbf{x} d\mathbf{y} e^{\beta K}, \end{aligned} \quad (\text{A16})$$

where  $K$  denotes the quadratic form in the exponent; constant terms have been absorbed into the normalization.

Collecting all contributions that scale extensively with  $N$ , we finally obtain

$$\mathbb{E}[Z^n] = \int \exp \left\{ N \left( -\beta \left[ \sum_a (\hat{m}_a m_a + \hat{u}_a u_a) + \sum_{a,b} (\hat{q}_{ab} q_{ab} + \hat{r}_{ab} r_{ab} + \hat{p}_{ab} p_{ab}) \right] + \frac{\beta}{2} \sum_a m_a^2 - \frac{\beta\gamma}{2} \sum_a u_a^2 \right. \right. \\ \left. \left. + \alpha \log \int d\mathbf{x} d\mathbf{y} e^{\beta K} + \log \int_{-i\infty}^{i\infty} d\phi \text{Tr } e^{\beta L} \right) \right\}. \quad (\text{A17})$$

Here,

$$L = \frac{1+\alpha\gamma}{2} \sum_a (\phi^a)^2 + \sqrt{\epsilon} \sum_a S^a \phi^a + \sum_a \hat{m}_a S^a + \sum_a \hat{u}_a \phi^a + \sum_{a,b} \hat{q}_{ab} S^a S^b \\ + \sum_{a,b} \hat{r}_{ab} S^a \phi^b + \sum_{a,b} \hat{p}_{ab} \phi^a \phi^b, \quad (\text{A18})$$

$$K = -\frac{i\gamma}{2\beta} \sum_a (x^a)^2 + \frac{i}{2\beta} \sum_a (y^a)^2 + \frac{i\gamma}{2} \sum_{a,b} q_{ab} x^a x^b + \frac{i\gamma}{2} \sum_{a,b} p_{ab} y^a y^b + i\gamma \sum_{a,b} r_{ab} x^a y^b. \quad (\text{A19})$$

The saddle-point equations follow from extremizing the exponent with respect to the order parameters and their conjugates, yielding

$$\hat{m}_a = m_a, \quad \hat{u}_a = -\gamma u_a, \quad (\text{A20})$$

$$m_a = \langle S^a \rangle_L, \quad u_a = \langle \phi^a \rangle_L, \quad (\text{A21})$$

$$\hat{q}_{ab} = \frac{i\alpha\gamma}{2} \langle x^a x^b \rangle_K, \quad \hat{r}_{ab} = i\alpha\gamma \langle x^a y^b \rangle_K, \quad \hat{p}_{ab} = \frac{i\alpha\gamma}{2} \langle y^a y^b \rangle_K, \quad (\text{A22})$$

$$q_{ab} = \langle S^a S^b \rangle_L, \quad r_{ab} = \langle S^a \phi^b \rangle_L, \quad p_{ab} = \langle \phi^a \phi^b \rangle_L, \quad (\text{A23})$$

where  $\langle \cdot \rangle_L$  and  $\langle \cdot \rangle_K$  denote averages with weights  $e^{\beta L}$  and  $e^{\beta K}$ , respectively.

For the RS reduction of the remaining Gaussian averages, it is convenient to use the following standard property of Gaussian variables. If  $z_1$  and  $z_2$  are independent standard normal variables, then  $az_1 + bz_2$  is distributed as  $\sqrt{a^2 + b^2} z$ , where  $z$  is a standard normal variable. This relation allows us to reduce the relevant two-dimensional Gaussian average to a one-dimensional one.

Finally, in the zero-temperature limit  $\beta \rightarrow \infty$ , one has  $q \rightarrow 1$  and  $\tanh(\beta \tilde{H}) \rightarrow \text{sgn}(\tilde{H})$ , which leads to the zero-temperature form of the saddle-point equations.

## Appendix B: Detailed calculation of AT line

We consider a one-step replica-symmetry-breaking (1RSB) perturbation around the RS saddle point. In the 1RSB ansatz, replica indices are grouped into blocks of size  $x \in [0, 1]$  (the Parisi breaking parameter). For each overlap, we introduce a subscript 1 when two replicas belong to the same block and a subscript 0 when they belong to different blocks. We then expand the saddle-point equations to first order in the deviations between the 1RSB and RS solutions, and determine whether the RS solution is stable against such perturbations. This procedure yields the de Almeida–Thouless (AT) stability condition.

For a pair of replica indices  $(a, b)$ , there are three cases:

1.  $a \neq b$  and  $a, b$  belong to the same block (e.g.  $\beta \hat{q}_1$ ),
2.  $a \neq b$  and  $a, b$  belong to different blocks (e.g.  $\beta \hat{q}_0$ ),
3.  $a = b$  (e.g.  $\beta \hat{q}_1 + \hat{\chi}_q$ ).

As an illustration, we focus on the part associated with the term  $K$ . After applying a Hubbard–Stratonovich transformation, we introduce auxiliary Gaussian variables  $\tilde{\mathbf{z}}$  and  $\mathbf{z}$  and obtain an expression of the form

$$\begin{aligned} & \mathbb{E}_{\mathbf{z} \sim \mathcal{N}(0, \Omega_1)} \left[ \left( \mathbb{E}_{\tilde{\mathbf{z}} \sim \mathcal{N}(0, \tilde{\Omega}_1)} \left[ \left( \int dy_1 dy_2 \exp \left( -\frac{i\gamma}{2} y_1^2 + \frac{i}{2} y_2^2 + \frac{i\gamma\beta}{2} \chi_q y_1^2 + \frac{i\gamma\beta}{2} \chi_p y_2^2 \right. \right. \right. \right. \right. \\ & \quad \left. \left. \left. \left. \left. \left. + i\gamma\beta \chi_r y_1 y_2 + \sqrt{\beta\gamma} (z_1 + \tilde{z}_1) y_1 + \sqrt{\beta\gamma} (z_2 + \tilde{z}_2) y_2 \right) \right)^x \right] \right)^{n/x} \right] \\ & \equiv \mathbb{E}_{\mathbf{z}} \left[ \left( \mathbb{E}_{\tilde{\mathbf{z}}} \left[ \left( \int dy \exp \left( -\frac{1}{2} \mathbf{y}^\top G \mathbf{y} + \mathbf{\Gamma}^\top \mathbf{y} \right) \right)^x \right] \right)^{n/x} \right], \end{aligned} \quad (B1)$$

where  $G$  and  $\mathbf{\Gamma}$  summarize the quadratic and linear terms in  $\mathbf{y}$ .

To extract the linear response with respect to the 1RSB perturbation, we need to distinguish whether a pair of replicas  $(a, b)$  belongs to the same block or to different blocks. The relevant contributions can be written schematically as follows. For case (1) (same block,  $a \neq b$ ),

$$\mathbb{E}_{\mathbf{z}} \left[ \left( \mathbb{E}_{\tilde{\mathbf{z}}} [F(\tilde{\mathbf{z}})^x] \right)^{\frac{n}{x}-1} \left( \mathbb{E}_{\tilde{\mathbf{z}}} [F(\tilde{\mathbf{z}})^{x-2} (F_1(\tilde{\mathbf{z}}))^2] \right) \right], \quad (B2)$$

whereas for case (2) (different blocks,  $a \neq b$ ),

$$\mathbb{E}_{\mathbf{z}} \left[ \left( \mathbb{E}_{\tilde{\mathbf{z}}} [F(\tilde{\mathbf{z}})^x] \right)^{\frac{n}{x}-2} \left( \mathbb{E}_{\tilde{\mathbf{z}}} [F(\tilde{\mathbf{z}})^{x-1} F_1(\tilde{\mathbf{z}})] \right)^2 \right], \quad (\text{B3})$$

with

$$F(\tilde{\mathbf{z}}) \equiv \int d\mathbf{y} e^{(\sim)}, \quad F_1(\tilde{\mathbf{z}}) \equiv \int d\mathbf{y} y_1 e^{(\sim)}. \quad (\text{B4})$$

For fixed  $\mathbf{z}$ , it is convenient to regard the tilted measure

$$P(\tilde{\mathbf{z}}) \equiv \frac{1}{\mathbb{E}_{\tilde{\mathbf{z}}} [F(\tilde{\mathbf{z}})^x]} \frac{F(\tilde{\mathbf{z}})^x}{\sqrt{(2\pi)^2 \det \tilde{\Omega}_1}} \exp \left( -\frac{1}{2} \tilde{\mathbf{z}}^\top \tilde{\Omega}_1^{-1} \tilde{\mathbf{z}} \right) \quad (\text{B5})$$

as the effective distribution of  $\tilde{\mathbf{z}}$ . Then the difference between case (1) and case (2) takes the form of a variance under  $P(\tilde{\mathbf{z}})$ , which implies

$$\beta(\hat{q}_1 - \hat{q}_0) = \frac{i\alpha\gamma}{2} \mathbb{E}_{\mathbf{z}} \left[ \text{Var}_{\tilde{\mathbf{z}}} \left[ \frac{1}{\sqrt{\beta\gamma}} \frac{\partial}{\partial \tilde{z}_1} \log F(\tilde{\mathbf{z}}) \right] \right]. \quad (\text{B6})$$

Similarly,

$$\beta(\hat{p}_1 - \hat{p}_0) = \frac{i\alpha\gamma}{2} \mathbb{E}_{\mathbf{z}} \left[ \text{Var}_{\tilde{\mathbf{z}}} \left[ \frac{1}{\sqrt{\beta\gamma}} \frac{\partial}{\partial \tilde{z}_2} \log F(\tilde{\mathbf{z}}) \right] \right], \quad (\text{B7})$$

$$\beta(\hat{r}_1 - \hat{r}_0) = i\alpha\gamma \mathbb{E}_{\mathbf{z}} \left[ \text{Cov}_{\tilde{\mathbf{z}}} \left[ \frac{1}{\sqrt{\beta\gamma}} \frac{\partial}{\partial \tilde{z}_1} \log F(\tilde{\mathbf{z}}), \frac{1}{\sqrt{\beta\gamma}} \frac{\partial}{\partial \tilde{z}_2} \log F(\tilde{\mathbf{z}}) \right] \right]. \quad (\text{B8})$$

The Gaussian integral over  $\mathbf{y} = (y_1, y_2)$  can be evaluated explicitly:

$$\begin{aligned} F(\tilde{\mathbf{z}}) &= \int dy_1 dy_2 \exp \left( -\frac{1}{2} \mathbf{y}^\top M \mathbf{y} + \sqrt{\beta\gamma} (z_1 + \tilde{z}_1)y_1 + \sqrt{\beta\gamma} (z_2 + \tilde{z}_2)y_2 \right) \\ &= \Delta^{-1/2} \exp \left( \frac{iA}{2} (z_1 + \tilde{z}_1)^2 + \frac{iB}{2} (z_2 + \tilde{z}_2)^2 + iC(z_1 + \tilde{z}_1)(z_2 + \tilde{z}_2) \right), \end{aligned} \quad (\text{B9})$$

where  $\Delta$  is the determinant factor and the coefficients are

$$A = -\frac{\beta}{\Delta} (1 + \gamma\beta\chi_p), \quad (\text{B10})$$

$$B = \frac{\gamma\beta}{\Delta} (1 - \beta\chi_q), \quad (\text{B11})$$

$$C = \frac{\gamma\beta^2}{\Delta} \chi_r. \quad (\text{B12})$$

Differentiating  $\log F$  with respect to  $\tilde{z}_1$  and  $\tilde{z}_2$  gives

$$\frac{\partial}{\partial \tilde{z}_1} \log F = iA\tilde{z}_1 + iC\tilde{z}_2 + iAz_1 + iCz_2, \quad (\text{B13})$$

$$\frac{\partial}{\partial \tilde{z}_2} \log F = iB\tilde{z}_2 + iC\tilde{z}_1 + iBz_2 + iCz_1. \quad (\text{B14})$$

Since  $z_1$  and  $z_2$  drop out when taking  $\text{Var}_{\mathbf{z}}$ , we obtain a closed linear relation between the deviations,

$$\hat{q}_1 - \hat{q}_0 = \frac{\alpha}{2\Delta^2} \left[ (1 + \gamma\beta\chi_p)^2 (q_1 - q_0) + \gamma^2\beta^2\chi_r^2 (p_1 - p_0) - 2\gamma\beta(1 + \gamma\beta\chi_p)\chi_r(r_1 - r_0) \right], \quad (\text{B15})$$

$$\hat{p}_1 - \hat{p}_0 = \frac{\alpha\gamma^2}{2\Delta^2} \left[ \beta^2\chi_r^2 (q_1 - q_0) + (1 - \beta\chi_q)^2 (p_1 - p_0) + 2\beta(1 - \beta\chi_q)\chi_r(r_1 - r_0) \right], \quad (\text{B16})$$

$$\begin{aligned} \hat{r}_1 - \hat{r}_0 &= \frac{\alpha\gamma}{\Delta^2} \left[ -\beta(1 + \gamma\beta\chi_p)\chi_r(q_1 - q_0) + \gamma\beta(1 - \beta\chi_q)\chi_r(p_1 - p_0) \right. \\ &\quad \left. + (-(1 + \gamma\beta\chi_p)(1 - \beta\chi_q) + \gamma\beta^2\chi_r^2)(r_1 - r_0) \right]. \end{aligned} \quad (\text{B17})$$

We now collect the deviations between the 1RSB and RS solutions into vectors

$$\mathbf{v} \equiv \begin{bmatrix} q_1 - q_0 \\ r_1 - r_0 \\ p_1 - p_0 \end{bmatrix}, \quad \hat{\mathbf{v}} \equiv \begin{bmatrix} \hat{q}_1 - \hat{q}_0 \\ \hat{r}_1 - \hat{r}_0 \\ \hat{p}_1 - \hat{p}_0 \end{bmatrix}.$$

The above relations can then be written compactly as

$$\hat{\mathbf{v}} = U \mathbf{v}. \quad (\text{B18})$$

Performing the same linearization for the single-site term  $L$ , we similarly obtain

$$\mathbf{v} = V \hat{\mathbf{v}}. \quad (\text{B19})$$

Composing the two relations yields closed equations for  $\mathbf{v}$  (or  $\hat{\mathbf{v}}$ ). The RS solution is locally stable if and only if the largest eigenvalue of  $UV$  (equivalently,  $VU$ ) is smaller than 1; otherwise the RS solution is unstable, which defines the AT instability condition.

### Appendix C: Replica Analysis at Optimal Parameters

We consider the case of

$$J' = \gamma((2 + \alpha)J - J^2). \quad (\text{C1})$$

This yields

$$\begin{aligned} Z &= \text{Tr} \exp \left( \frac{\beta}{2} \mathbf{S}^\top J' \mathbf{S} \right) \\ &= \text{Tr} \exp \left( \frac{\beta\gamma(2 + \alpha)}{2} \mathbf{S}^\top J \mathbf{S} - \frac{\beta\gamma}{2} \mathbf{S}^\top J^2 \mathbf{S} \right). \end{aligned} \quad (\text{C2})$$

Here,

$$\begin{aligned}
\text{Tr} \exp \left( -\frac{\beta\gamma}{2} \mathbf{S}^\top J^2 \mathbf{S} \right) &= \text{Tr} \exp \left( -\frac{\beta\gamma}{2} (J\mathbf{S})^2 \right) \\
&= \int \prod_i d\phi_i \text{Tr} \exp \left( -\frac{\beta\gamma}{2} \sum_i \phi_i^2 + i\beta\gamma \boldsymbol{\phi}^\top J\mathbf{S} \right) \\
&= \int_{-i\infty}^{i\infty} \prod_i d\phi_i \text{Tr} \exp \left( \frac{\beta\gamma}{2} \sum_i \phi_i^2 + \beta\gamma \boldsymbol{\phi}^\top J\mathbf{S} \right). \tag{C3}
\end{aligned}$$

thus introducing auxiliary variables. Proceeding as in Appendix A, we obtain

$$m = \mathbb{E}_{\mathbf{z} \sim \mathcal{N}(0, \Omega_2)} \left[ \tanh \beta\gamma \left( \hat{m} + z_1 - \frac{(\hat{r}_1 - \alpha)(\hat{u} + z_2)}{2\hat{p}_1 + 1} \right) \right] \tag{C4}$$

$$q_0 = \mathbb{E}_{\mathbf{z} \sim \mathcal{N}(0, \Omega_2)} \left[ \tanh^2 \beta\gamma \left( \hat{m} + z_1 - \frac{(\hat{r}_1 - \alpha)(\hat{u} + z_2)}{2\hat{p}_1 + 1} \right) \right] \tag{C5}$$

$$q_1 = 1 - q_0 \tag{C6}$$

$$u = -\frac{1}{2\hat{p}_1 + 1} ((-\alpha + \hat{r}_1) \mathbb{E}[\tanh] + \hat{u}) \tag{C7}$$

$$p_1 = -\frac{1}{\beta\gamma(2\hat{p}_1 + 1)} + \frac{(\hat{r}_1 - \alpha)^2 (1 - \mathbb{E}[\tanh^2])}{(2\hat{p}_1 + 1)^2} \tag{C8}$$

$$p_0 = \frac{1}{(2\hat{p}_1 + 1)^2} ((-\alpha + \hat{r}_1)^2 \mathbb{E}[\tanh^2] + 2(-\alpha + \hat{r}_1)(\hat{u} \mathbb{E}[\tanh] + \mathbb{E}[z_2 \tanh]) + \hat{u}^2 + 2\hat{p}_0) \tag{C9}$$

$$r_1 = -\frac{1}{2\hat{p}_1 + 1} (-\alpha + \hat{r}_1) (1 - \mathbb{E}[\tanh^2]) \tag{C10}$$

$$r_0 = -\frac{1}{2\hat{p}_1 + 1} ((-\alpha + \hat{r}_1) \mathbb{E}[\tanh^2] + \hat{u} \mathbb{E}[\tanh] + \mathbb{E}[z_2 \tanh]). \tag{C11}$$

$$\hat{m} = (2 + \alpha)m + u \quad (C12)$$

$$\hat{u} = m \quad (C13)$$

$$\hat{q}_1 = \frac{\alpha}{2\Delta}(\beta\gamma p_1 + 2 + \alpha) \quad (C14)$$

$$\hat{q}_0 = \frac{\alpha}{2\Delta^2}((\beta\gamma p_1 + 2 + \alpha)^2 q_0 + 2(\beta\gamma p_1 + 2 + \alpha)(1 - \beta\gamma r_1)r_0 + (1 - \beta\gamma r_1)^2 p_0) \quad (C15)$$

$$\hat{p}_1 = \frac{\alpha\beta\gamma}{2\Delta}q_1$$

$$\hat{p}_0 = \frac{\alpha}{2\Delta^2}((1 - \beta\gamma r_1)^2 q_0 + 2\beta\gamma q_1(1 - \beta\gamma r_1)r_0 + \gamma^2\beta^2 q_1^2 p_0) \quad (C16)$$

$$\hat{r}_1 = \frac{\alpha}{\Delta}(1 - \beta\gamma r_1) \quad (C17)$$

$$\begin{aligned} \hat{r}_0 = \frac{\alpha}{\Delta^2} & \left( (\beta\gamma p_1 + 2 + \alpha)(1 - \gamma\beta r_1)q_0 + \beta\gamma q_1(\beta\gamma p_1 + 2 + \alpha)r_0 \right. \\ & \left. + (1 - \gamma\beta r_1)^2 r_0 + \beta\gamma q_1(1 - \gamma\beta r_1)p_0 \right). \end{aligned} \quad (C18)$$

are obtained. By taking  $\beta\gamma \rightarrow \infty$  so that  $\beta\gamma q_1 = C, \beta\gamma p_1 = E, \beta\gamma r_1 = F$ ,

$$m = \text{erf}\left(\frac{\hat{m} - A\hat{u}}{\delta}\right) \quad (C19)$$

$$C = \frac{2}{\delta\sqrt{\pi}} \exp\left(-\frac{(\hat{m} - A\hat{u})^2}{\delta^2}\right) \quad (C20)$$

$$u = -\frac{1}{2\hat{p}_1 + 1}((- \alpha + \hat{r}_1)m + \hat{u}) \quad (C21)$$

$$E = -\frac{1}{2\hat{p}_1 + 1} + \frac{(\hat{r}_1 - \alpha)^2 C}{(2\hat{p}_1 + 1)^2} \quad (C22)$$

$$p_0 = \frac{1}{(2\hat{p}_1 + 1)^2}(( - \alpha + \hat{r}_1)^2 + 2(- \alpha + \hat{r}_1)(\hat{u}m + C(\hat{r}_0 - 2\hat{p}_0 A)) + \hat{u}^2 + 2\hat{p}_0) \quad (C23)$$

$$F = -\frac{1}{2\hat{p}_1 + 1}(- \alpha + \hat{r}_1)C \quad (C24)$$

$$r_0 = -\frac{1}{2\hat{p}_1 + 1}(- \alpha + \hat{r}_1 + \hat{u}m + C(\hat{r}_0 - 2\hat{p}_0 A)). \quad (C25)$$

$$\hat{m} = (2 + \alpha)m + u \quad (C26)$$

$$\hat{u} = m \quad (C27)$$

$$\hat{q}_1 = \frac{\alpha}{2\Delta}(E + 2 + \alpha) \quad (C28)$$

$$\hat{q}_0 = \frac{\alpha}{2\Delta^2}((E + 2 + \alpha)^2 + 2(E + 2 + \alpha)(1 - F)r_0 + (1 - F)^2p_0) \quad (C29)$$

$$\hat{p}_1 = \frac{\alpha}{2\Delta}C \quad (C30)$$

$$\hat{p}_0 = \frac{\alpha}{2\Delta^2}((1 - F)^2 + 2C(1 - F)r_0 + C^2p_0) \quad (C31)$$

$$\hat{r}_1 = \frac{\alpha}{\Delta}(1 - F) \quad (C32)$$

$$\begin{aligned} \hat{r}_0 = \frac{\alpha}{\Delta^2} & \left( (E + 2 + \alpha)(1 - F) + C(E + 2 + \alpha)r_0 \right. \\ & \left. + (1 - F)^2r_0 + C(1 - F)p_0 \right). \end{aligned} \quad (C33)$$

Also,  $A, \Delta, \delta, \Delta_2$  are

$$A = \frac{\hat{r}_1 - \alpha}{2\hat{p}_1 + 1} \quad (C34)$$

$$\Delta = -C(E + 2 + \alpha) + (1 - F)^2 \quad (C35)$$

$$\delta = \sqrt{\frac{(2\hat{q}_0 + \sqrt{\Delta_2} - A\hat{r}_0)^2 + (\hat{r}_0 - 2A\hat{p}_0 - A\sqrt{\Delta_2})^2}{\hat{q}_0 + \hat{p}_0 + \sqrt{\Delta_2}}} \quad (C36)$$

$$\Delta_2 = 4\hat{q}_0\hat{p}_0 - \hat{r}_0^2. \quad (C37)$$

Using these saddle-point equations to plot the overlap  $m$ , the result is as shown in Fig. 8. The memory capacity is approximately  $\alpha_c \simeq 0.42$ , which agrees with the capacity obtained in [8].

- [1] J. J. Hopfield, Neural networks and physical systems with emergent collective computational abilities., *Proceedings of the national academy of sciences* **79**, 2554 (1982).
- [2] D. J. Amit, H. Gutfreund, and H. Sompolinsky, Storing infinite numbers of patterns in a spin-glass model of neural networks, *Physical Review Letters* **55**, 1530 (1985).
- [3] J. J. Hopfield, D. I. Feinstein, and R. G. Palmer, ‘unlearning’ has a stabilizing effect in collective memories, *Nature* **304**, 158 (1983).
- [4] F. Crick and G. Mitchison, The function of dream sleep, *Nature* **304**, 111 (1983).

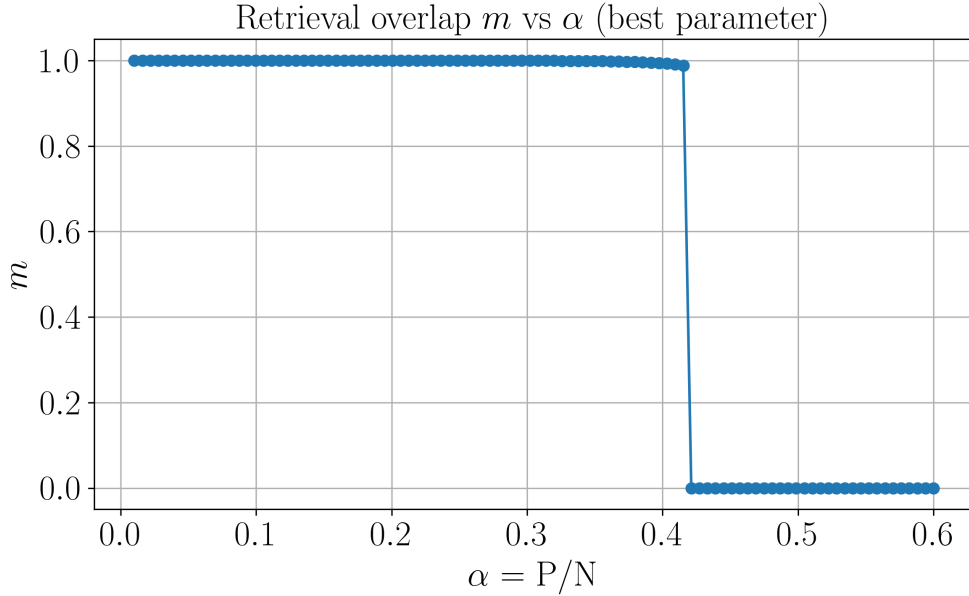


FIG. 8. Overlap  $m$  vs  $\alpha$  at best parameters

- [5] A. Fachechi, E. Agliari, and A. Barra, Dreaming neural networks: forgetting spurious memories and reinforcing pure ones, *Neural Networks* **112**, 24 (2019).
- [6] E. Agliari, F. Alemanno, A. Barra, and A. Fachechi, Dreaming neural networks: rigorous results, *Journal of Statistical Mechanics: Theory and Experiment* **2019**, 083503 (2019).
- [7] M. Benedetti, L. Carillo, E. Marinari, and M. Mézard, Eigenvector dreaming, *Journal of Statistical Mechanics: Theory and Experiment* **2024**, 013302 (2024).
- [8] K. Nokura, Unlearning in the paramagnetic phase of neural network models, *Journal of Physics A: Mathematical and General* **29**, 3871 (1996).
- [9] M. Mézard, G. Parisi, and M. A. Virasoro, *Spin glass theory and beyond: An Introduction to the Replica Method and Its Applications*, Vol. 9 (World Scientific Publishing Company, 1987).
- [10] J. R. de Almeida and D. J. Thouless, Stability of the sherrington-kirkpatrick solution of a spin glass model, *Journal of Physics A: Mathematical and General* **11**, 983 (1978).